Mechanism of bright red emission in Si nanoclusters

Article *in* Nanotechnology · October 2008

DOI: 10.1088/0957-4484/19/39/395401 · Source: PubMed

9 authors, including:

S. Dhara
Indira Gandhi Centre for Atomic Research
277 PUBLICATIONS **4,172** CITATIONS
SEE PROFILE

Chin-Pei Chen
National Yang Ming University
20 PUBLICATIONS **1,128** CITATIONS
SEE PROFILE

C. David
Indira Gandhi Centre for Atomic Research
73 PUBLICATIONS **444** CITATIONS
SEE PROFILE

Baldev Raj
Indira Gandhi Centre for Atomic Research
919 PUBLICATIONS **18,386** CITATIONS
SEE PROFILE

Nanotechnology **19** (2008) 395401 (5pp) doi:10.1088/0957-4484/19/39/395401

Mechanism of bright red emission in Si nanoclusters

S Dhara[1,5], C-Y Lu[2], K G M Nair[1], K-H Chen[2,3], C-P Chen[2], Y-F Huang[4], C David[1], L-C Chen[4] and Baldev Raj[1]

[1] Materials Science Division, Indira Gandhi Centre for Atomic Research, Kalpakkam 603 102, India
[2] Institute of Atomic and Molecular Sciences, Academia Sinica, Taipei 106, Taiwan
[3] Center for Condensed Matter Sciences, National Taiwan University, Taipei 106, Taiwan
[4] Department of Electro-Optical Engineering, National Taipei University of Technology, Taipei 106, Taiwan

E-mail: dhara@igcar.gov.in

Received 6 June 2008, in final form 20 July 2008
Published 8 August 2008
Online at stacks.iop.org/Nano/19/395401

Abstract

A bright photoluminescence around 1.7 eV is observed for post-annealed samples of 1 MeV Si^{2+} implanted in an SiO_2 matrix. A super-linear power dependence of photoluminescence intensity accompanied by pulse shortening under continuous wave laser excitation is recorded without any spectral narrowing. An emission process comprised of an initial non-radiative recombination (time constant ∼280–315 ps) of excited carriers in the defect states in SiO_2 matrices to the conduction band minima of nc-Si, followed by a slower process of radiative recombination in the direct band transition for nc-Si along with a non-radiative Auger recombination (time constant ∼2.67 ns) is proposed.

S Supplementary data are available from stacks.iop.org/Nano/19/395401

(Some figures in this article are in colour only in the electronic version)

1. Introduction

Integrating light with Si is one of the longstanding problems in semiconductor technology. Various methodologies have been devised for improving the efficiency of the radiative recombination in the indirect bandgap bulk crystalline (c-) Si. The majority of efforts are in the form of nanocrystalline (nc-) Si [1–5], along with other systems, e.g. erbium-doped Si-rich oxides [6, 7], Si/SiO_2 superlattices [8], Si/SiGe quantum cascade structures [9], surface-textured bulk Si [10], dislocation-engineered strained Si [11] and silicon on insulator (SOI) as rib waveguide for Raman lasing [12]. Early studies on porous silicon (PS) sparked some hope for light emission from nc-Si (500–900 nm) [1]. An increased quantum efficiency (QE) of ∼1–3% is reported for PS with respect to the measured value of 10^{-4}–10^{-5}% for c-Si. Recent advances in the growth of nc-Si widened the emission range from the blue to the red wavelength region of visible light. A higher QE of photoluminescence (PL) intensity by one order (∼10%) than that for PS is also reported for a single nc-Si [5]. Formation of a direct bandgap in nc-Si, as well as widening of it due to quantum confinement of carriers, are well conceived [3, 8]. However, the mechanism of luminescence in the nc-Si system, including that of the PS, is not very well understood. According to the present perception, the observed luminescence is explained in terms of electron–hole (e–h) pair recombination with a role for $Si–SiO_x$ interface states [1, 2, 13]. Defect states, created during the growth of nc-Si by ion implantation in a silica matrix, is also thought to be responsible for the luminescence process [4]. The role of the $Si–SiO_x$ interface in the observed photoluminescence of nc-Si is always emphasized. As a matter of fact, the nc-Si grown in a c-Al_2O_3 substrate fails to report any observable PL intensity [14].

It is still a daunting task to improve the applicability of light-emitting silicon structures for the successful achievement of stimulated emission and light amplification, which is a necessary condition for the realization of an Si-based semiconductor laser. Optical gain in the red spectral region

[5] Author to whom any correspondence should be addressed. Present address: Department of Electrical Engineering, Institute of Innovations and Advanced Studies, National Cheng Kung University, Tainan 701, Taiwan.

is first reported in the nc-Si embedded in an SiO_2 matrix, indicating the possibility of population inversion of the radiative states associated with the Si–SiO_2 interface [2]. Later, a stimulated blue emission without any spectral narrowing is reported for the radiative transmission at extremely high (100 MW cm^{-2}) excitation density [4]. Most recently, a Raman laser with a significant spectral narrowing is reported in the SOI waveguide using optical gain in the silica matrix [12].

We report here the room temperature (RT) PL properties of nc-Si grown by Si ion implantation in both amorphous (a-) and c-SiO_2 matrices and the subsequent annealing process. A super-linear power dependence of luminescence study under continuous wave (cw) excitation is observed in the radiative recombination process accompanied by pulse shortening. A possible population inversion is suggested for the observed emission process with a competitive Auger recombination process.

2. Experimental details

1 MeV Si^{2+} is implanted in a-SiO_2 matrix for various fluences of 1×10^{16}–1×10^{17} cm^{-2} at RT using a 1.7 MV Tandetron accelerator. The implanted samples are annealed isothermally at 1373 K for 10 h in H_2–Ar (8% H_2) gas. Another sample is prepared with a fixed fluence of 1×10^{17} cm^{-2} in (0001) oriented c-SiO_2 substrate and similar annealing conditions. SRIM calculation shows a range of 1 MeV Si^{2+} in silica is ∼1.2 μm and a straggling of 0.85 μm [15]. Thus the active layer is expected to be ∼1 μm. Regarding the choice of annealing atmosphere, we must state here that, while the majority of the reports use N_2 as ambient [16–19], use of pure Ar is also reported [20] for similar luminescence properties for nc-Si in SiO_x matrices. Though the role of H_2 in other nanostructures is reported, namely for the reversal of heterojunction formation in SiC nanowires (in the core) coated with a thin layer of SiO_2 to a structure with SiC coated on an SiO_2 core [21], we do not anticipate such modification in the deeply embedded nanostructures. H_2 here is to ensure complete prohibition of oxidation in Ar ambient where oxygen as an impurity may always be present. No qualitative change in the PL property is reported even for nc-Si in porous SiO_x matrices [22]. Cross-sectional transmission electron microscopy (JEOL 2000FX, XTEM) is studied for typical nanocluster imaging. The PL studies are performed using the excitation of the 325 nm line of a cw He–Cd laser in a double subtractive triple monochromator (Juvin-Yvon T64000 spectrograph). A liquid N_2 cooled 'back-thinned' charge-coupled device (CCD) detector (QE ∼ 80%) is used for the detection of luminescence intensity. Time-resolved PL measurements are carried out using a 375 nm pulsed diode laser (LDH-P-C-375) with a pulse width <70 ps, with different power densities at 40 MHz.

3. Results and discussion

Figure 1(a) shows the PL spectra for samples implanted at various fluences. The second-order peak ∼1.91 eV, corresponding to the excitation line, is also observed along

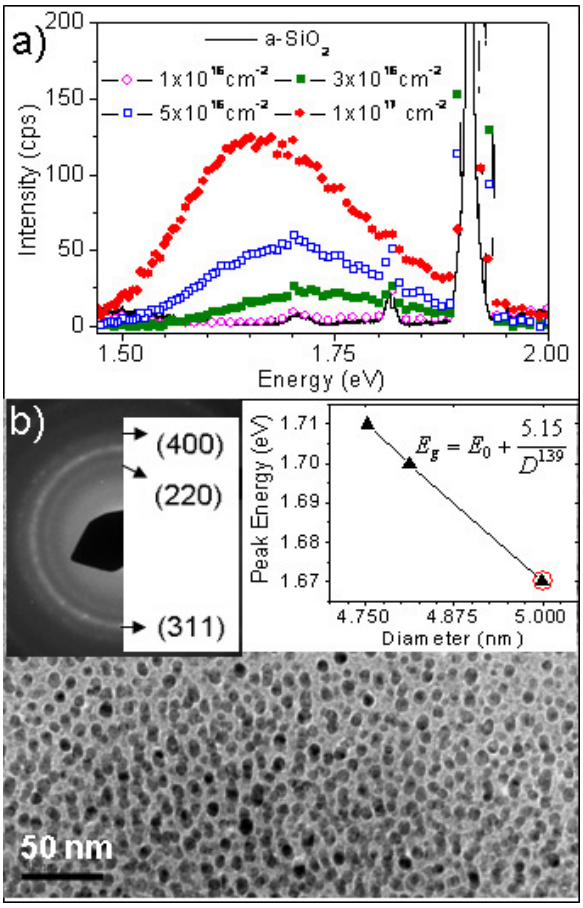

Figure 1. (a) The PL spectra (intensities normalized in counts per second) are shown for samples implanted at various fluences and annealed at 10 h. (b) A typical XTEM image of uniformly sized ∼5 nm clusters is shown for the sample grown with a fluence of 1×10^{17} cm^{-2}. The left inset shows the ring diffraction pattern with various planes corresponding to nc-Si. The right inset shows correlation between average diameter and PL peak energy (scattered points with filled triangles) according to the inscribed empirical formula. The continuous line is a guide to the eyes. The circle is the experimentally observed data for the sample grown with a fluence of 1×10^{17} cm^{-2}.

with NBO-defect related peaks at 1.70 and 1.81 eV [23]. No appreciable change in the luminescence intensity is observed for samples implanted below the fluence of 3×10^{16} cm^{-2}. A blueshift of the PL peak is observed with decreasing fluence. Small clusters are expected with less nucleation density of the precipitated clusters at low fluences. A detailed discussion regarding cluster growth mechanism of the ion implanted sample may be read in the recent review article [24]. A typical XTEM image shows a fairly uniform cluster with diameter ∼5 nm (figure 1(b)) for the 10 h annealed sample grown at a fluence of 1×10^{17} cm^{-2}. Electron diffraction pattern (top left inset in figure 1(b)) shows the ring pattern corresponding to the (220), (311) and (400) planes of Si nanocrystallites [25]. An XTEM study also shows (supplementary figure S1 available at stacks.iop.org/Nano/19/395401) an active sample thickness of ∼1 μm. An observed direct bandgap energy (E_g) of 1.67 eV is plotted (circled; top right inset in (figure 1(b))), for known average value of cluster diameter (D) ∼ 5 nm. Other

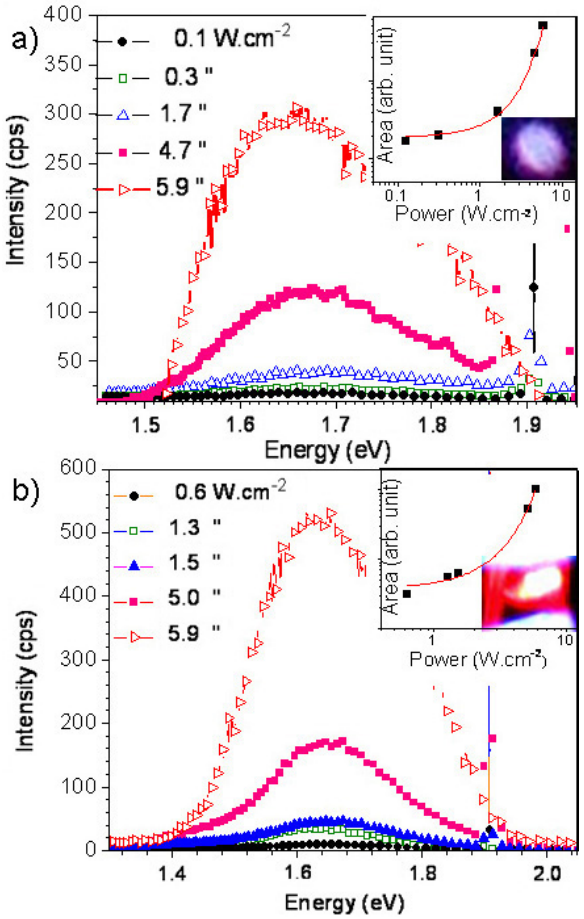

Figure 2. The power-dependent PL spectra (intensities normalized in counts per second) are shown for samples implanted in (a) a-SiO_2 and (b) c-SiO_2 substrates at a fluence of 1×10^{17} cm^{-2} and annealed at 10 h. Respective insets show the nonlinear log–log plots of PL integrated intensity (area under curves) with varying power density. Pictures with the bright luminescence are also shown in the respective insets.

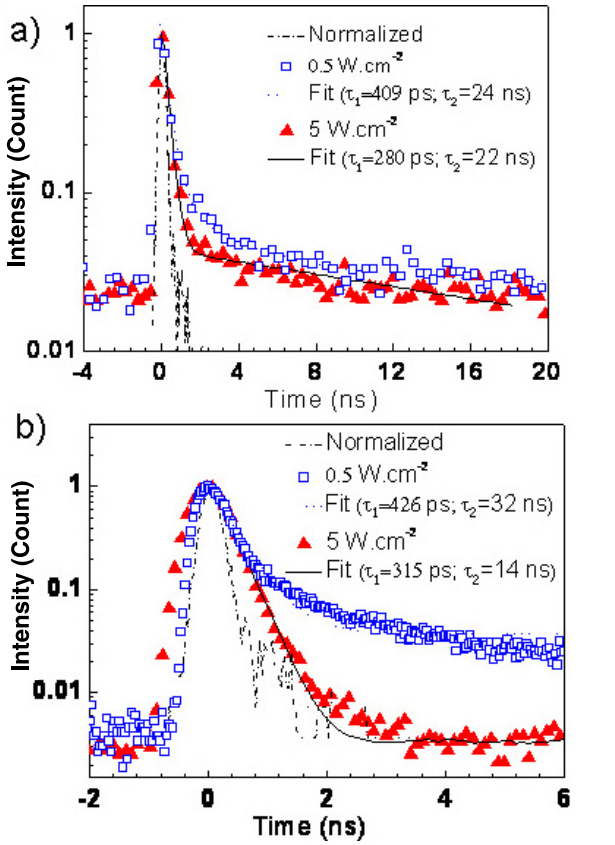

Figure 3. Room temperature PL decay processes for samples grown in (a) a-SiO_2 and (b) c-SiO_2 substrates at a fluence of 1×10^{17} cm^{-2} and annealed at 10 h. Scattered points are the experimental data, the dashed lines are the instrumental decay and the continuous lines are double-exponential fits. The spectra are collected at peak energy with different power densities. The fitting parameters with decay constants are also inscribed.

measured peak energies of the samples, grown with fluences up to 3×10^{16} cm^{-2}, are also plotted as scattered points (filled triangle) for their expected sizes. The empirical formula of $E_g = E_0 + 5.15/D^{1.39}$ [3] is used with the indirect bandgap E_0 (= 1.12 eV) for bulk Si.

Figures 2(a) and (b) show the power-dependent PL studies for the post-annealed sample grown in both a- and c-SiO_2 with a fluence of 1×10^{17} cm^{-2}. Insets in figure 2 show a nonlinear log–log plot indicating super-linear power dependence of PL intensity integrated over the area (supplementary figure S2 available at stacks.iop.org/Nano/19/395401 for normal scale plot). The estimated power dependence is 1.4 and 1.2 for samples grown in a- and c-SiO_2, respectively. Even though the nc-Si sample is spread $\sim$1 μm across the depth, a multiple reflection in the quartz matrix might have increased the active layer thickness affecting the observed intensity (supplementary figure S3 available at stacks.iop.org/Nano/19/395401 for expected interference pattern). Hardly any spectral change (neither a shift in PL peak position nor spectral narrowing) is observed even up to the highest cw excitation power density of 5.9 W cm^{-2}. However, the spectra show a narrowing effect for samples grown in c-SiO_2 substrates as compared to that observed for the samples grown in a-SiO_2 substrates. The bright features of PL intensities corresponding to the highest incident power density are also shown in the insets of figures 2(a) and (b).

A time-resolved PL measurement for both the post-annealed samples grown in a- and c-SiO_2 matrices at a fluence of 1×10^{17} cm^{-2} are shown in figures 3(a) and (b), respectively. The data are collected for a part of the spectrum corresponding to the peak (1.67 eV) energy for different power densities. The PL decay curves are not single exponentials. The decay processes of PL peak can be satisfactorily fitted with a double-exponential function with time constants of τ_1 and τ_2, as mentioned in the insets for samples grown in a-SiO_2 and c-SiO_2. A pulse shortening is observed when measured at a higher power density of 5 W cm^{-2} and it is most prominent in the case of a sample grown in c-SiO_2. Similar time scales are reported earlier for nc-Si grown in a silica matrix by ion implantation technique under pulsed excitation [4, 26]. We must state that the commonly reported decay time constant of microseconds is missing in our study. Generally, the fast component is related to the increasing laser pumping fluence or long active length accumulating large compensating

defects [27]. The slow emission represents a spontaneous emission in the radiative recombination process. An amplified spontaneous emission (ASE) is useful for a stimulated process using the optical gain of the medium, but it is always not a necessary condition for observing such a phenomenon. For an example, a stimulated emission is reported for the nc-Si embedded in a silica matrix in the absence of a slow emission process [4]. As a matter of fact, we get a slower process of 14–22 ns at a highest power density than those reported in [4]. In the high optical gain of a silica matrix, this apparently fast recombination process can influence the observed strong emission process.

As a possible mechanism, excited carriers from the valence band of nc-Si ($VB_{nc\text{-}Si}$) are injected into the intermediate defect states, in the silica matrix related to the Si–O interface states (figure 4(a)). These states are produced during the sample preparation process. Absorption peaks ∼1.74–1.8 eV for the nc-Si sample embedded in amorphous and crystalline silica matrices strongly support the presence of such defect states (figure 4(b)). This feature of the near-infrared absorption band is caused by a Si=O interface [28]. As predicted by theory [29] and inferred from the experiment [28], these defect states are formed at the interface between the nc-Si and the SiO_2 matrix. Optically excited carriers thermalize non-radiatively at a very rapid rate (280–315 ps) to the next lower energy state of the conduction band minima corresponding to nc-Si ($CB_{nc\text{-}Si}$). Finally, the carriers recombine with holes in VB_{nc-Si} either radiatively and/or non-radiatively (figure 4(a)). In the case of a broad defect band (as indicated in the absorption spectra (figure 4(b))) each system will emit only in a narrow frequency regime, under the consideration that one or a few e–h pairs can recombine radiatively (14–22 ns at highest power density) in a simultaneous fashion within each individual system. As a consequence, the spectral line will be broadened due to the different neighborhood of each system and PL emission spectrum is not likely to change even with the increase in the excitation intensity. However, the amount of defects created in the irradiation process may have an influence upon the spectral narrowing. The observed spectral narrowing effect, as described earlier (figure 2), can be well conceived in this model with an expected fewer degree of defects or defect states in the crystalline matrix than those in the amorphous matrix. Additionally, all the states which relax radiatively may automatically lead to an inversion of population. Here we consider isolated systems, each of which consists of three levels. These states can be occupied by one electron in the $VB_{nc\text{-}Si}$, the higher excited states where absorption takes place and the intermediate CB_{nc-Si} as depicted in figure 4(a). The assignments can be referred to the already reported defect states and consequent stimulated emission in the pulsed excitation for the nc-Si embedded in silica by the ion implantation technique [4].

A super-linear power dependence of PL accompanied by a pulse shortening, with no spectral narrowing of PL spectra, needs a further appraisal of the above-described emission process. As mentioned earlier, a radiative emission process from the $CB_{nc\text{-}Si}$ to the $VB_{nc\text{-}Si}$ can involve a competitive non-radiative process (figure 4(a)). One such process that can be

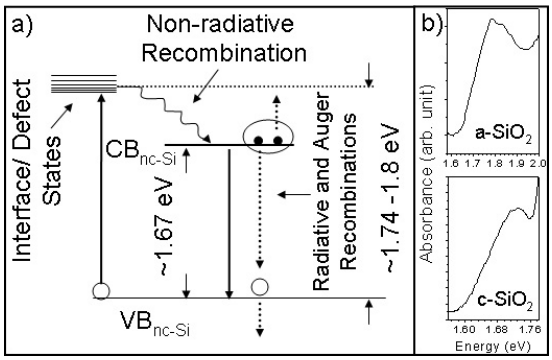

Figure 4. (a) A schematic band diagram of the overall luminescence process. (b) Typical absorbance spectra for the sample implanted in different SiO_2 matrices at a fluence of 1×10^{17} cm^{-2} and annealed at 10 h.

imagined is the Auger recombination process. In fact, the presence of Auger recombination is also reported for nc-Si in silica matrices [29]. For nc-Si with a diameter 5 nm, the Auger recombination time ($\tau_A = 1/n^2C$; where C is the Auger coefficient and n is the photoexcited electron density) is calculated to be 2.67 ns with $n = 2/V$ (V being the nanocrystal volume with a couple of e–h pairs) and $C = 4 \times 10^{-31}$ cm^6 s^{-1} [30]. The calculated time constant is within the range of the measured time constants of 14–22 ns in the present study. As a matter of fact, Auger recombination with a similar time constant ($\tau_A \sim 3$ ns) in addition to a stimulated emission process is successfully used to describe a luminescence process in nc-Si under pulsed excitation [28].

4. Conclusion

In conclusion, a super-linear power dependence of the bright red emission ∼1.67 eV for nc-Si accompanied with a pulse shortening is observed under a continuous wave excitation. However, the nonlinearity fails to show any significant spectral narrowing. The luminescence process is proposed to be based on the competition between radiative and non-radiative relaxation processes in isolated luminescence centers. The proposed mechanism is supported with the energetic and different recombination time constants derived from experimental observations.

References

[1] Vial J C, Bsiesy A, Gaspard F, Herino R, Ligeon M, Muller F, Romestain R and Macfarlane R M 1992 *Phys. Rev.* B **45** 14171
[2] Pavesi L, Negro L D, Mazzoleni C, Franzo G and Priolo F 2000 *Nature* **408** 440
[3] Ledoux G, Gong J, Huisken F, Guillois O and Reynaud C 2002 *Appl. Phys. Lett.* **80** 4834
[4] Luterova K, Pelant I, Mikulskas I, Tomasiunas R, Muller D, Grob J-J, Rehspringer J-L and Honerlage B 2002 *J. Appl. Phys.* **91** 2896
[5] Valenta J, Juhasz R and Linnros J 2002 *Appl. Phys. Lett.* **80** 1070
[6] Lourenço M A, Gwilliam R M and Homewood K P 2007 *Appl. Phys. Lett.* **91** 141122

[7] Izeddin I, Klik M A J, Vinh N Q, Bresler M S and Gregorkiewicz T 2007 *Phys. Rev. Lett.* **99** 077401
[8] Lockwood D J, Lu Z H and Baribeau J M 1996 *Phys. Rev. Lett.* **76** 539
[9] Bates R *et al* 2003 *Appl. Phys. Lett.* **83** 4092
[10] Trupke T, Zhao J, Wang A, Corkish R and Green M 2003 *Appl. Phys. Lett.* **82** 2996
[11] Ng W L, Lourenc M A, Gwilliam R M, Ledain S, Shao G and Homewood K P 2001 *Nature* **410** 192
[12] Rong H, Liu A, Jones R, Cohen O, Hak D, Nicolaescu R, Fang A and Paniccia M 2005 *Nature* **433** 292
[13] Gole J L, Dudel F P, Grantier D and Dixon D A 1997 *Phys. Rev.* B **56** 2137
[14] Yerci S, Serincan U, Dogan I, Tokay S, Genisel M, Aydinli A and Turan R 2006 *J. Appl. Phys.* **100** 074301
[15] Ziegler J F, Biersack J P and Littmark U 1985 *The Stopping and Range of Ions in Solids* (New York: Pergamon) (http://www.srim.org/)
[16] Valenta J, Lalic N and Linnros J 2004 *Appl. Phys. Lett.* **84** 1459
[17] Khriachtchev L, Rasanen M, Novikov S and Sinkkonen J 2001 *Appl. Phys. Lett.* **79** 1249
[18] Linnros J, Lalic N, Galeckas A and Grivickas V 1999 *J. Appl. Phys.* **86** 6128
[19] Shimizu-Iwayama T, Kurumado N, Hole D E and Townsend P D 1998 *J. Appl. Phys.* **83** 6018
[20] Qian C, Zhang Z X, Zhang F and Lin C L 2007 *Mater. Res. Soc. Symp. Proc.* **1020** GG07–19
[21] Rummeli M, Borowiak-Palen E, Gemming T, Huczko A, Knupfer M, Cudzilo S, Kalenczuk R J and Pichler T 2005 *Synth. Met.* **153** 349
[22] Bineva I, Nesheva D, Aneva Z, Levi Z, Raptis C, Hofmeister H and Stavrev S 2003 *J. Mater. Sci. Mater. Electron.* **14** 799
[23] Zyubin A S, Glinka Y D, Mebel A M, Lin S H, Hwang L P and Chen Y T 2002 *J. Chem. Phys.* **116** 281
[24] Dhara S 2007 *Crit. Rev. Solid State Mater. Sci.* **32** 1
[25] *JCPDS—The International Centre for Powder Diffraction* Card Number 27-1402
[26] Trojanek F, Neudert K, Bittner M and Maly P 2005 *Phys. Rev.* B **72** 075365
[27] Pavesi L 2003 *J. Phys.: Condens. Matter* **15** R1169
[28] Wolkin M V, Jorne J, Fauchet P M, Allan G and Delerue C 1999 *Phys. Rev. Lett.* **82** 197
[29] Degoli E and Ossicini S 2000 *Surf. Sci.* **470** 32
[30] Linnros J 1998 *J. Appl. Phys.* **84** 284